Int J Clin Exp Med 2020;13(2):901-908
www.ijcem.com /ISSN:1940-5901/IJCEM0101725

Original Article

The diagnostic value of high-resolution, susceptibility-weighted imaging for cerebral amyloid angiopathy with cerebral microbleed

Cheng Ma[1*], Yumei Wang[2*], Li Liu[3], Qingtao Ma[2], Ming Yang[4], Xiaodong Li[5]

[1]Department of Medical Imaging, Zibo City Linzi District People's Hospital, Zibo, Shandong Province, China; [2]Department of Imaging, Zaozhuang Hospital of Zaozhuang Mining Group, Zaozhuang, Shandong Province, China; [3]Department of Imaging, Maternity and Child Health Care of Zaozhuang, Zaozhuang, Shandong Province, China; [4]Department of Imaging, The People's Hospital of Shanting District, Zaozhuang, Shandong Province, China; [5]CT Room, The People's Hospital of Pingyi County, Pingyi, Shandong Province, China. [*]Equal contributors and co-first authors.

Received August 31, 2019; Accepted January 3, 2020; Epub February 15, 2020; Published February 28, 2020

Abstract: Objective: This study aimed to explore the application value of high-resolution, susceptibility-weighted imaging (SWI) for the early diagnosis of cerebral amyloid angiopathy (CAA) with cerebral microbleed (CMB). Methods: A total of 50 patients highly suspected of CAA were enrolled in this study. Enhanced brain CTs indicated that the volume of CMB was smaller than 10 mm. Differences in image quality, the number of hemorrhagic foci detected, the distribution of the hemorrhages, and the amount of hemorrhage were compared between conventional magnetic resonance imaging (MRI) sequences and the SWI sequence, so as to assess the diagnostic value of SWI for CAA with CMB. Results: Compared with those of the conventional sequences, the SWI sequence showed a significantly higher qualified rate of image quality and number of hemorrhagic foci detected, as well as a larger amount of hemorrhage ($P<0.05$), but there was no difference in the distribution of hemorrhage ($P>0.05$). Conclusion: High-resolution SWI, which is highly sensitive to intracranial hemorrhage and even to micro-hemorrhagic foci, has high image quality in the early diagnosis of CAA with CMB, so it has a high diagnostic value and can become the first choice for the early diagnosis of CAA.

Keywords: Susceptibility weighted imaging, cerebral amyloid angiopathy, cerebral microbleed

Introduction

Cerebral amyloid angiopathy (CAA) is a cerebral hemorrhagic disease that commonly occurs among elderly people. Significantly increasing with age, its incidence is also related to gene mutation, β-amyloid protein deposition, metabolic disorders of apolipoprotein E, and abnormal inflammatory responses [1, 2]. According to published data, in elderly patients, CAA-induced spontaneous cerebral hemorrhage accounts for more than 20% of all intracranial hemorrhages; at least 30-50% of people over 60 years old suffer from CAA-related cerebral hemorrhage, and at least 20-30% of them may experience a secondary cognitive decline [3, 4]. Therefore, CAA and its secondary cerebral hemorrhage have become major diseases affecting the health of the elderly. It's difficult to diagnose the disease since there are few typical symptoms in the early stages of CAA, and no typical signs of neurological defects, even if it is accompanied by cerebral microbleed (CMB). Without specific biochemical indices and typical medical imaging, currently, CAA is comprehensively evaluated using the patient's medical history, the clinical signs, and the imaging examinations [5].

Although it is highly sensitive to early hemorrhagic foci, brain computed tomography (CT) has a low positive rate of diagnosing CMB and intralobular hemorrhage [6]. Magnetic resonance imaging (MRI), whose conventional sequences consist of a T1 weighted image (T1WI), T2WI, fluid attenuated inversion recov-

ery (FLAIR), and diffusion weighted imaging (DWI), is highly sensitive to the diagnosis of soft tissue lesions. In the T2*-weighted gradient-echo (T2*-GRE) sequence, a circular low-density area with uniform and consistent signals can be usually detected, with diameters smaller than 10 mm but mostly around 2-5 mm, which is called CMB [7]. As for CMB, the area of the hemorrhagic foci is small, without any obvious edema around it and without any clinical symptoms. However, recent studies have suggested that CMB is not only an early and typical sign of microangiopathy related to the deposition of specific proteins and the structural destruction of vascular walls, but it is also a high-risk factor for rebleeding and hemorrhage after anticoagulation, which is commonly found in the elderly population and in patients with CAA, leukoencephalopathy, or cerebral small vessel diseases [8, 9]. Based on the T2*-GRE sequence, susceptibility weighted imaging (SWI) has an extremely high sensitivity to intracerebral hemorrhage using advanced three-dimensional fusion and flow compensation in all directions, with longer echo times, higher resolution, and a thinner reconstruction [10]. This imaging method detects hemorrhagic foci within 2 h, showing images earlier than CT [11]. To explain the main mechanism, in addition to a strong magnetic sensitivity effect, SWI has a high recognition capability for deoxyhemoglobin and hemosiderin massively produced in red blood cells after hemorrhage, so it can distinguish a hemorrhagic focus from the surrounding tissue by fusing the amplitude diagram and the phase diagram [12]. At present, SWI has been widely applied in the diagnosis of ischemic and hemorrhagic stroke, brain trauma, cerebrovascular malformation, brain tumors and degenerative brain diseases. However, there are few studies on SWI in CAA and CAA with CMB. Therefore, the application value of high-resolution SWI for the early diagnosis of CAA with CMB was explored in this study.

Materials and methods

General information

Altogether 50 patients highly suspected of CAA and admitted to The People's Hospital of Pingyi County from May 2018 to May 2019 were retrospectively studied. Inclusion criteria: (1) Patients aged 50-80 years. (2) Patients with stable conditions and localized cerebral microhemorrhagic foci detected by brain CT. (3) Patients could be accompanied by a cognitive decline that did not affect the clinical treatment and research. (4) Patients had MRI sequence images that could be analyzed. (5) Patients signed the informed consent form and had complete clinical data. Exclusion criteria: (1) patients complicated with another cerebral hemorrhage such as a subarachnoid hemorrhage, traumatic cerebral hemorrhage, or an aneurysmal rupture-induced hemorrhage; (2) patients with a hemorrhage after anticoagulation or primary hematological diseases; (3) patients with Alzheimer's disease or vascular dementia who could not cooperate in this study; (4) patients with nutritional deficiency diseases or autoimmune diseases; (5) patients with contraindications to MRI or claustrophobia.

Methods

Patients lay flat on the examining table, with their heads fixed. A 1.5T superconducting magnetic resonance scanner (Siemens, Germany) with Loop4 coils was used. Conventional sequence scanning was conducted first. The fast turbo spin echo sequence was used in T1WI and T2WI. The specific parameters were as follows: T1 axis view (time of repetition (TR) = 195.0 ms, time of echo (TE) = 4.8 ms), T1 sagittal view (TR = 550.0 ms, TE = 8.4 ms), T2 axis view (TR = 4000.0 ms, TE = 98.0 ms), matrix = 256 * 256, field of view (FOV) = 70 mm * 70 mm, layer thickness = 2 mm, layer spacing = 0.2 mm, the number of layers = 20; FLAIR axis (TR = 8200.0 ms, TE = 84.0 ms), layer thickness = 6.0 mm, layer spacing = 1.2 mm. The hemorrhagic focus was designated as the region of interest after it was found. Then, the sequence was adjusted to the SWI sequence. The parameters were as follows: TR = 49.0 ms, TE = 40.0 ms, flip angle = 15°, FOV = 230 mm * 230 mm, matrix = 256 * 256, layer thickness = 2.0 mm, layer spacing = 0.4 mm, the number of layers = 20. After the images were transmitted to the post-processing workstation, the SWI processing software provided by the instrument was used to form a fusion diagram and a minimum density projection drawing, so as to calculate the volume of hemorrhage = the hematoma area of each layer * (layer thickness + layer spacing) * 1/2.

Table 1. Analysis of the baseline data

Item	
Number of cases (n)	50
Gender (male/female)	26/24
Age (year)	56-79 (62.3±8.6)
Hypertension (n, %)	16 (32.0)
Diabetes (n, %)	6 (12.0)
Hyperlipidemia (n, %)	5 (10.0)
Coronary heart disease (n, %)	7 (14.0)
Stroke (n, %)	5 (10.0)
Cerebral microhemorrhage volume (m^3)	2-8 (5.2±2.3)

Table 2. Analysis of baseline data (n, %)

Imaging method	Conventional MRI sequences (n=50)	SWI sequence (n=50)	χ^2	P
Grade 1	18 (36.0)	28 (56.0)		
Grade 2	24 (48.0)	20 (40.0)		
Grade 3	8 (16.0)	2 (4.0)		
The qualified rate	42 (84.0)	48 (96.0)	4.000	0.046

Note: MRI, magnetic resonance imaging; SWI, susceptibility weighted imaging.

MRI was performed by radiologists who had been professionally trained and had worked for at least 2 years. Three doctors jointly completed the image acquisition and analysis of the 50 patients. At least 2 doctors had to reach an agreement on the diagnostic results.

Outcome measures

Differences in image quality, the number of hemorrhagic foci detected, the distribution of the hemorrhages, and the amount of hemorrhage were compared between the conventional MRI sequences (T1WI, T2WI, FLAIR, and DWI) and the SWI sequence, so as to assess the diagnostic value of SWI for CAA with CMB. The image quality was classified based on a Three-Grade classification [13]. Grade 1 indicated that the image was very clear and accurately displayed the range of hemorrhagic foci and the changes of the adjacent tissue. Grade 2 indicated that the image was relatively clear and basically displayed the site and the area of the hemorrhage. Although there were a few artifacts in the surrounding tissue, the pathological features could still be analyzed. Grade 3 indicated that the image was very unclear, so the site and the amount of the hemorrhage could not be diagnosed. The images in Grades 1 and 2 had qualified quality.

Statistical methods

SPSS 20.0 was used for the statistical analysis. The data conforming to a normal distribution were expressed as the means ± standard deviations and compared using a *t* test. The count data were expressed as the number of cases/percentage and compared using an χ^2 test. Bilateral 0.50 was used as the significance level and P<0.05 indicated a statistically significant difference.

Results

Analysis of baseline data

Among the 50 patients, there were 26 males and 24 females, aged 56-79 years with an average age of (62.3±8.6) years. There were 16 cases of hypertension, 6 of diabetes, 5 of hyperlipidemia, 7 of coronary heart disease, and 5 of stroke. An enhanced brain CT indicated that the volume of the CMB was smaller than 10 mm, specifically 2-8 mm, with an average volume of (5.2±2.3) mm. See **Table 1**.

Analysis of the image quality

The qualified rate of image quality detected by the SWI was significantly higher than the rate detected by the conventional MRI sequences (P<0.05). With a qualified rate of 96.0%, SWI was found to meet the needs of the clinical diagnosis of CMB. See **Table 2** and **Figure 1**.

Comparison of the number of hemorrhagic foci and the amount of hemorrhage

The number of hemorrhagic foci detected by SWI was significantly higher than the number detected by conventional MRI sequences, and the amount of hemorrhage was larger than the amount detected by conventional MRI sequences (both P<0.05). See **Table 3** and **Figure 2**.

Comparison of the distribution of hemorrhagic foci

There was no difference in the distribution of hemorrhagic foci between that detected by SWI

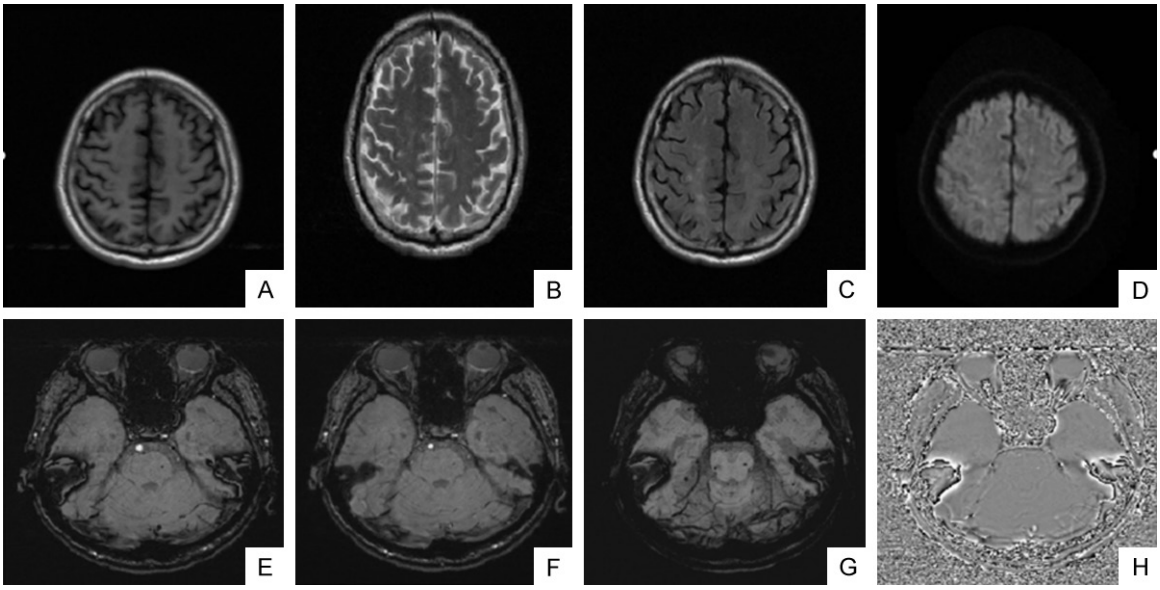

Figure 1. Typical case 1 image by conventional MRI sequences (T1WI, T2WI, FLAIR, and DWI) and SWI sequence. A: T1WI; B: T2WI; C: FLAIR; D: DWI; E: SWI; F: MAG; G: MIP; H: PHA. Typical case 1, male, 68 years old, was admitted to our hospital, because of recurrent spontaneous cerebral hemorrhage for 6 months and progressive cognitive decline for 3 months. He had hypertension for 5 years but no diabetes, coronary heart disease, and cerebral infarction, so he was orally administrated antihypertensive drugs for treatment. He had spontaneous cerebral hemorrhages about 3 times with the amount smaller than 5 m^3. The patient had no significant sign of neurological deficit. The hemorrhagic focus was basically absorbable after conservative treatment with drugs. Conventional MRI sequences showed that there were a few hemorrhagic foci in the temporo-parietal junction, but no focus in the subcortex, basal ganglia, brainstem, and subarachnoid space. The T2-FLAIR images clearly showed that the hemorrhagic focus was on the right side. SWI could use its own image fusion technology to post-process MAG, MIP, and PHA, with an emphasis on displaying the region of interest. MRI, magnetic resonance imaging; T1WI, T1 weighted image; FLAIR, fluid attenuated inversion recovery; DWI, diffusion weighted imaging; SWI, susceptibility weighted imaging; MAG, magnitude imaging; MIP, minimum intensity projection; PHA, phase image.

Table 3. Comparison of the number of hemorrhagic foci and the hemorrhagic volume ($\bar{x}$ ± sd)

Imaging method	Conventional MRI sequences (n=50)	SWI sequence (n=50)	t	P
The number of hemorrhagic foci	1.4±0.5	1.8±0.6	3.968	0.025
Hemorrhagic volume (m^3)	5.0±2.4	5.6±2.3	4.562	0.011

Note: MRI, magnetic resonance imaging; SWI, susceptibility weighted imaging.

and by conventional MRI sequences (P>0.05). The hemorrhage site of patients with CAA was mainly in the lobes of the brain, and less in the cortex and subcortex, thalamus, brainstem, basal ganglia, and subarachnoid space. See **Tables 4** and **5**.

Discussion

Conventional MRI sequences use SE imaging technologies and machines to emit radiofrequency pulses at 90° and then another focused pulse at 180° at certain intervals, so as to eliminate the phase effect caused by uneven magnetic fields and to generate T2 relaxation signals. The principle of SWI is that in the T2*-GRE sequence, a pair of dephasing gradient magnetic fields with opposite polarities are directly combined with rephasing gradient magnetic fields, so as to generate a phase dispersion effect [14]. SWI is highly sensitive to the local magnetic fields of hemorrhage and shows hypointensity [15].

This study explored the application values of conventional MRI sequences and the SWI sequence on CAA with CMB. The results showed that compared with the conventional MRI sequences, the SWI sequence showed significantly a higher qualified rate of image quality and a larger number of hemorrhagic foci detected, as well as larger amount of hemorrhage, but

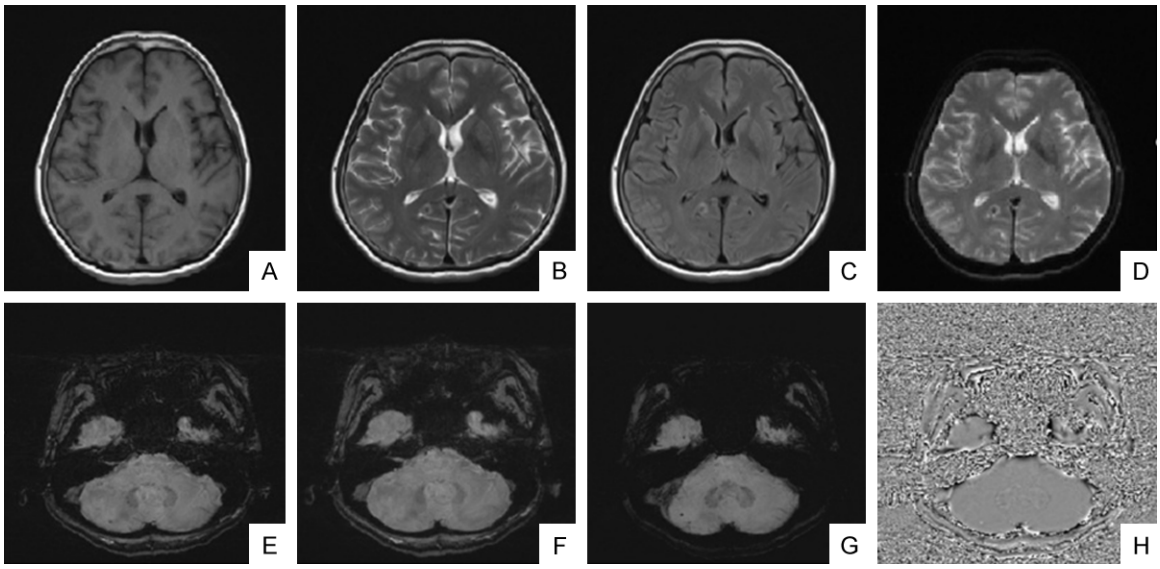

Figure 2. Typical case 2 image by conventional MRI sequences (T1WI, T2WI, FLAIR, and DWI) and SWI sequence. A: T1WI; B: T2WI; C: FLAIR; D: DWI; E: SWI; F: MAG; G: MIP; H: PHA. Typical case 2, female, 75 years old, was mainly characterized by cerebral small blood vessel hemorrhages accompanied by mild neurological dysfunction, which was caused by unexplained factors. The patient had diabetes for 10 years but no hypertension, so she was orally administrated hypoglycemic agents and injected with insulin. She had poor blood glucose control and diabetic retinopathy. After admission, she was initially confirmed to have CAA through a brain CT. The site of the hemorrhage was in the right occipital lobe, and the amount of hemorrhage was smaller than 8 m^3. The hemorrhagic focus was basically absorbable after conservative treatment with drugs. The amount of hemorrhage detected by SWI was larger than the amount detected by conventional MRI sequences. MRI, magnetic resonance imaging; T1WI, T1 weighted image; FLAIR, fluid attenuated inversion recovery; DWI, diffusion weighted imaging; SWI, susceptibility weighted imaging; MAG, magnitude imaging; MIP, minimum intensity projection; PHA, phase image; CAA, cerebral amyloid angiopathy; CT, computed tomography.

Table 4. Comparison of the distribution of hemorrhagic foci (n, %)

Imaging method	Conventional MRI sequences (n=50)	SWI sequence (n=50)	χ^2	P
Total number of hemorrhagic foci	73	90		
Site			0.563	0.452
Cerebral lobe	65 (89.0)	73 (81.1)		
Cortex and subcortex	5 (6.8)	10 (11.1)		
Thalamus, brainstem and basal ganglia	3 (4.1)	6 (6.7)		
Subarachnoid space	0	1 (1.1)		

Note: MRI, magnetic resonance imaging; SWI, susceptibility weighted imaging.

Table 5. Comparison of the distribution of hemorrhagic foci in the cerebral lobe (n, %)

Imaging method	Conventional MRI sequences (n=50)	SWI sequence (n=50)	χ^2	P
Total number of hemorrhagic foci in cerebral lobe	65	73	1.952	0.162
Temporoparietal lobe	28 (43.1)	29 (39.7)		
Occipital lobe	20 (30.8)	23 (31.5)		
Frontal lobe	17 (26.1)	21 (28.8)		

Note: MRI, magnetic resonance imaging; SWI, susceptibility weighted imaging.

there was no difference in the distribution of hemorrhages. The main factors causing changes in magnetic fields after a hemorrhage are blood metabolites, venules, and the effect of

iron deposition. The large amount of deoxyhemoglobin in the venules can easily cause an inhomogeneity change in the magnetic fields. Both significantly shortened the GRE time in the SWI sequence, and the greater phase difference between the blood vessels at the focus and in the surrounding tissue make the local venule structure clearly displayed. This is also the main reason why SWI can clearly display blood vessels at the hemorrhage site [16, 17].

The difference between SWI and GRE is the significant changes in the imaging parameters, such as shorter TR values, longer TE, thinner layer thicknesses, shorter layer spacing, a significantly shorter total scanning time, a change from 2D imaging to 3D imaging, and a higher resolution. All of these improve the definition and accuracy of hemorrhage imaging [18]. Therefore, at present, SWI has been widely applied in the diagnosis of ischemic and hemorrhagic stroke, brain trauma, cerebrovascular malformation, brain tumors, degenerative brain diseases, and cerebral degenerative diseases [19, 20].

Taking advantage of three-dimensional fusion, flow compensation in all directions, longer echo time, higher resolution, and thinner reconstruction, SWI has an extremely high sensitivity to intracerebral hemorrhage. This imaging method detects hemorrhagic foci within 2 h, showing images earlier than CT. After a hemorrhage, deoxyhemoglobin and hemosiderin are massively produced in the red blood cells. And SWI has a high recognition capability for them as well as a strong magnetic sensitivity effect on them. So it can distinguish a hemorrhagic focus from the surrounding tissue by fusing the amplitude diagram and the phase diagram. Magnitude image (MAG) post-processing mainly uses diffusion-weighted imaging to form color images, and it measures isotropic and anisotropic values that are called apparent diffusion coefficients [21]. Phase images are filtered using gradients to remove unnecessary field effects, so as to generate phase masks, which is called phase image (PHA) technology [22]. Then, the intensity diagram is enhanced by the phase mask, and the minimum intensity projection is carried out on the relatively adjacent layers, which is called minimum intensity projection (MIP) technology [23]. The data and image information collected after multi-layer post-processing significantly improves the definition and contrast of the images, with an extremely high sensitivity to veins, hemorrhage, and iron deposition [24, 25].

SWI mainly shows hypointensity accompanied by a central isointensity in the acute phase of intracerebral hemorrhage, and hypointensity accompanied by a little central hyperintensity in the subacute phase. In the chronic phase, intermediate intensity and peripheral annular hypointensity are shown, which is the characteristic of hemosiderosis [26, 27]. In SWI, CAA is usually manifested as a multiple well-defined and spotted hypointensity within the brain parenchyma, with a diameter smaller than 5 mm and a short continuity at multiple layers [28, 29]. SWI is more sensitive and accurate than traditional MRI sequences and GRE in the diagnosis of cerebral hemorrhagic diseases such as CAA with CMB, so it can clearly display the venules. Although it may exaggerate the risk of hemorrhage, it can better exclude all possible hemorrhagic diseases.

In summary, high-resolution SWI, which is highly sensitive to intracranial hemorrhage and even to micro-hemorrhagic foci, has high image quality in the early diagnosis of CAA with CMB, so it has a high diagnostic value and can become the first choice for the early diagnosis of CAA.

Disclosure of conflict of interest

None.

Address correspondence to: Xiaodong Li, CT Room, The People's Hospital of Pingyi Country, No. 7 Jinhua Road, Development Zone, Pingyi 273300, Shandong Province, China. Tel: +86-15266662677; Fax: +86-0539-4689088; E-mail: lixiaodong88xd@163.com

References

[1] Cong L. Research status of cerebral amyloid angiopathy. Journal of Apoplexy and Nervous Diseases 2017; 34: 954-956.

[2] Reijmer YD, van Veluw SJ and Greenberg SM. Ischemic brain injury in cerebral amyloid angiopathy. J Cereb Blood Flow Metab 2016; 36: 40-54.

[3] Zheng CY, Wang CQ, Ren Y, Xiang K and Xu GY. MRI findings of cerebrovascular amyloidosis cerebral hemorrhage. Neural Injury and Functional Reconstruction 2018; 13: 40-41.

[4] Wang X, Wang X and Zhang LM. Study of beta-amyloid protein in cerebrovascular diseases. Journal of Brain and Nervous Diseases 2018; 26: 450-453.
[5] Zhu CY, Liu HC, He H and Liu XQ. Evaluating cerebral endothelial dysfunction induced by amyloid based on the time series model. Journal of China Pharmaceutical University 2018; 49: 456-462.
[6] Zhou H, Liu JC, You Y, Luo GH, Xie PH, Yang J, Dong YL and Qing WP. Study on application of high-resolution magnetic resonance imaging in diagnosing cerebral amyloid angiopathy complicating ischemic stroke. Journal of Modern Medicine 2017; 33: 18-20, 24.
[7] Cai H, Lin ZM, Dding DB and Yang XW. Application of magnetic susceptibility weighted imaging in detection of acute cerebral infarction with cerebral microhemorrhage. China Practical Medical 2017; 12: 62-64.
[8] McCarthy RC and Kosman DJ. Iron transport across the blood-brain barrier: development, neurovascular regulation and cerebral amyloid angiopathy. Cell Mol Life Sci 2015; 72: 709-727.
[9] Wang XP, He JJ and Hu HQ. Diagnostic value of magnetic sensitive weighted imaging for microhemorrhage in the brain. Image Technology 2019; 31: 54-55.
[10] Wu ZF, Lu JC, Li GZ and Zhou LX. Clinical value of magnetic susceptibility weighted imaging in the diagnosis of cerebral microhemorrhage. Guangxi Medical Journal 2019; 41: 1040-1041, 1045.
[11] Zhao SF. Diagnostic value of magnetic susceptibility weighted imaging in small amount of cerebral hemorrhage. Chinese Journal of Medical Device 2019; 32: 48-49.
[12] Kirshner HS and Bradshaw M. The inflammatory form of cerebral amyloid angiopathy or "cerebral amyloid angiopathy-related inflammation" (CAARI). Curr Neurol Neurosci Rep 2015; 15: 54.
[13] Hu XH. 3.0T susceptibility weighted imaging in the diagnosis of intracranial cavernous hemangioma and venous hemangioma. Journal of Imaging Research and Medical Applications 2019; 3: 33-35.
[14] Jing YP, Fan QL, Luo B, Pei XH, Xu XF, Yao LD, Xin X, Zhang Y and Cheng JL. Study on the diagnostic value of MRI plain scan combined with SWI for intracranial micro hemorrhagic disease. Journal of Practical Medical Imaging 2018; 19: 386-389.
[15] Guo CF, Zhang T and Song TJ. Diagnostic value of 3.0T magnetic sensitivity weighted imaging in brain diseases. Journal of Imaging Research and Medical Applications 2018; 2: 88-90.
[16] Zhou H, Liu JC, Xie PH, You Y, Luo GH, Yang J and Qing WP. Comparison of diagnostic values between magnetic susceptibility weighted imaging and routine MRI in patients with cerebral amyloid angiopathy-related hemorrhage. Journal of Jilin University(Medicine Edition) 2017; 43: 1042-1046.
[17] Huang WQ, Lin HN, Lin Q and Tzeng CM. Susceptibility weighted imaging (swi) recommended as a regular magnetic resonance diagnosis for vascular dementia to identify independent idiopathic normal pressure hydrocephalus before ventriculo-peritoneal (V-P) shunt treatment: a case study. Front Neurol 2019; 10: 262.
[18] Yanai K, Ishida Y, Nishido H, Miyamoto S, Yamazaki K and Hoya K. Multiple cerebral hemorrhagic lesions depicted by susceptibility-weighted imaging in a patient with down syndrome: case report. J Stroke Cerebrovasc Dis 2019; 28: e37-e38.
[19] Skalski KA, Kessler AT and Bhatt AA. Hemorrhagic and non-hemorrhagic causes of signal loss on susceptibility-weighted imaging. Emerg Radiol 2018; 25: 691-701.
[20] Renard D. Cerebral microbleeds: a magnetic resonance imaging review of common and less common causes. Eur J Neurol 2018; 25: 441-450.
[21] Charidimou A, Martinez-Ramirez S, Reijmer YD, Oliveira-Filho J, Lauer A, Roongpiboonsopit D, Frosch M, Vashkevich A, Ayres A, Rosand J, Gurol ME, Greenberg SM and Viswanathan A. Total magnetic resonance imaging burden of small vessel disease in cerebral amyloid angiopathy: an imaging-pathologic study of concept validation. JAMA Neurol 2016; 73: 994-1001.
[22] Kida H, Satoh M, Ii Y, Fukuyama H, Maeda M and Tomimoto H. Detection of cerebral amyloid angiopathy by 3-T magnetic resonance imaging and amyloid positron emission tomography in a patient with subcortical ischaemic vascular dementia. Psychogeriatrics 2017; 17: 70-72.
[23] Cheng AL, Batool S, McCreary CR, Lauzon ML, Frayne R, Goyal M and Smith EE. Susceptibility-weighted imaging is more reliable than T2*-weighted gradient-recalled echo MRI for detecting microbleeds. Stroke 2013; 44: 2782-2786.
[24] Li L, Liu MS, Li GQ, Zheng Y, Guo TL, Kang X and Yuan MT. Susceptibility-weighted imaging in thrombolytic therapy of acute ischemic stroke. Chinese Medical Journal 2017; 130: 2489-2497.
[25] Liu S, Utriainen D, Chai C, Chen Y, Wang L, Sethi SK, Xia S and Haacke EM. Cerebral microbleed detection using Susceptibility Weight-

ed Imaging and deep learning. Neuroimage 2019; 198: 271-282.

[26] Di Ieva A, Lam T, Alcaide-Leon P, Bharatha A, Montanera W and Cusimano MD. Magnetic resonance susceptibility weighted imaging in neurosurgery: current applications and future perspectives. J Neurosurg 2015; 123: 1463-1475.

[27] Tóth A, Berente Z, Bogner P, Környei B, Balogh B, Czeiter E, Amrein K, Dóczi T, Büki A and Schwarcz A. Cerebral microbleeds temporarily become less visible or invisible in acute susceptibility weighted magnetic resonance imaging: a rat study. J Neurotrauma 2019; 36: 1670-1677.

[28] Sparacia G, Agnello F, La Tona G, Iaia A, Midiri F and Sparacia B. Assessment of cerebral microbleeds by susceptibility-weighted imaging in Alzheimer's disease patients: a neuroimaging biomarker of the disease. Neuroradiol J 2017; 30: 330-335.

[29] Liu Y, Liu J, Liu HH, Liao YJ, Cao L, Ye B and Wang W. Investigation of cerebral iron deposition in aged patients with ischemic cerebrovascular disease using susceptibility-weighted imaging. Ther Clin Risk Manag 2016; 12: 1239-1247.